Available online at www.sciencedirect.com
SCIENCE DIRECT
Journal of APPLIED MATHEMATICS AND MECHANICS
ELSEVIER
www.elsevier.com/locate/jappmathmech
Journal of Applied Mathematics and Mechanics 69 (2005) 649–664

THE AXISYMMETRIC NOSE SHAPE OF MINIMUM WAVE DRAG FOR GIVEN SIZE AND VOLUME†

N. L. YEFREMOV, A. N. KRAIKO and K. S. P'YANKOV

Moscow

email: akraiko@ciam.ru

(*Received* 4 *October* 2004)

Within the limits of Newton's formula, a solution of the problem of designing axisymmetric nose shapes that minimize wave drag for given volume and maximum admissible size is presented. The solution is obtained both in the slender-body approximation and in the complete formulation (without assuming a small angle between the axis of the body and the tangent to its contour). In both formulations, the optimum contours, besides a two-sided extremum segment, may contain a cylindrical generator – a boundary extremum segment with respect to the maximum admissible radial coordinate. In addition, in the complete formulation the optimum contours may include a leading or trailing flat end – a boundary extremum segment in the sense of both the longitudinal coordinate and the limit of applicability of Newton's formula. Determination of the drag coefficient of the nose shapes designed using numerical integration of the equations of the axisymmetric flow of an ideal gas confirmed the advantages of convex configurations. In the same approximation, the drag of optimum nose shapes (within the limits of Newton's formula) with concave segments may exceed the drag of equivalent cones. The formulation of the variational problem modified for such cases (in particular, with the fixed specification of the volume replaced by a lower bound) yields Newton's solution with a free volume.

1. THE OPTIMUM NOSE SHAPES IN THE SLENDER-BODY APPROXIMATION

Consider the problem of designing an axisymmetric nose shape which, when the pressure p at the surface of a body of fixed base radius R, fixed length L and fixed volume Ω is determined by Newton's formula, has the minimum wave drag D. As in [1], the problem will first be solved in the slender-body approximation. The solution constructed in [1] is incomplete, because for given Ω and relative thickness $\tau = R/L$ the equations and conditions obtained there permit the design of optimum nose shapes only over a quarter of the range of values of the coefficient $C_\Omega = \Omega/(\pi R^2 L)$.

Newton's formula [1–3] gives the pressure on the nose shape (*if* in Fig. 1a) as

$$p = p_\infty + \rho_\infty V_\infty^2 \sin^2\theta = p_\infty + \frac{q}{1+x'^2} \approx p_\infty + \frac{q}{x'^2}, \quad q = \rho_\infty V_\infty^2 \tag{1.1}$$

where ρ is the density, V is the velocity, $x = x(r)$ is the equation of the generator, $x' = dx/dr$, and the subscript ∞ indicates the parameters of the free stream directed along the x axis. The part of the formula for the pressure is written in the thin-boy approximation ($x'^2 \gg 1$).

For the coefficient C_Ω and the wave drag coefficient C_d of a slender nose shape, using formula (1.1) we have ($\xi' = d\xi/d\eta$)

$$C_\Omega \equiv \frac{\Omega}{\pi R^2 L} = \frac{1}{R^2 L}\int_0^R x' r^2 dr = \int_0^1 \xi' \eta^2 d\eta$$

†*Prikl. Mat. Mekh.* Vol. 69, No. 5, pp. 723–742, 2005.
0021–8928/$—see front matter.
doi: 10.1016/j.jappmathmech.2005.09.001

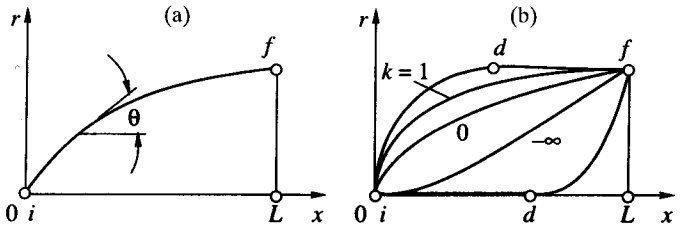

Fig. 1

$$C_d \equiv \frac{D}{\pi q R^2} = \frac{2}{qR^2}\int_0^R (p - p_\infty) r dr = \frac{2}{R^2}\int_0^R \frac{r dr}{1 + x'^2} \approx 2\tau^2 \int_0^1 \frac{\eta d\eta}{\xi'^2} \tag{1.2}$$

$$\xi = \frac{x}{L}, \quad \eta = \frac{r}{R}, \quad \tau = \frac{R}{L}$$

The variation of the Lagrange functional is found to be

$$\Phi = \frac{C_d}{2\tau^2} + \lambda C_\Omega = \int_0^1 \left(\frac{\eta}{\xi'^2} + \lambda \xi' \eta^2\right) d\eta$$

$$\delta\Phi = \int_0^1 \left[\left(\frac{2\eta}{\xi'^3} - \lambda\eta^2\right)' \delta\xi + \frac{3\eta}{\xi'^4}(\delta\xi')^2\right] d\eta + \left(\lambda\eta^2 - \frac{2\eta}{\xi'^3}\right)\delta\xi \Big|_i^f \tag{1.3}$$

where λ is a contact Lagrange multiplier, the prime denotes differentiation with respect to η, and $\delta\xi$ and $\delta\xi'$ are the variations of ξ and ξ' – the differences of the varied and unvaried functions for fixed η. For given coordinates of the end points $\delta\xi_i = \delta\xi_f = 0$. For fixed C_Ω and τ the variations of Φ and C_d have the same sign, and by formula (1.3) the necessary conditions for a minimum of C_d become

$$\left(\frac{2\eta}{\xi'^3} - \lambda\eta^2\right)' = 0, \quad \frac{3\eta}{\xi'^4} \geq 0$$

The second condition (Legendre's condition) is satisfied for all generators, while the first, after integrating and solving for ξ', reduces to the following equation (C is a constant of integration)

$$\xi' = (2\eta)^{1/3}/(C + \lambda\eta^2)^{1/3} \tag{1.4}$$

By the definition of ξ and η we have $\xi(0) = 0$ and $\xi(1) = 1$. Integrating Eq. (1.4) talking these conditions into account, we obtain the equation of the extremal *if* in the form

$$\xi = \frac{I(\eta, k)}{I(1, k)}, \quad \xi' \equiv \frac{d\xi}{d\eta} = \frac{\eta^{1/3}}{I(1, k)(1 - k\eta^2)^{1/3}}, \quad k = -\frac{\lambda}{C}$$

$$I(\eta, k) = \int_0^\eta \frac{\zeta^{1/3} d\zeta}{(1 - k\zeta^2)^{1/3}} = 2I_0(\eta, k) - \frac{3}{4}(1 - k\eta^2)^{2/3}\eta^{4/3} \tag{1.5}$$

$$I_0(\eta, k) = \int_0^\eta (1 - k\zeta^2)^{2/3} \zeta^{1/3} d\zeta$$

By formulae (1.2) and (1.5)

$$C_\Omega = I_\Omega(k), \quad C_d = \tau^2 I_d(k) \tag{1.6}$$

$$I_\Omega(k) = \frac{1}{I(1, k)}\int_0^1 \frac{\eta^{7/3} d\eta}{(1 - k\eta^2)^{1/3}} = \frac{1}{kI(1, k)}\left[I_0(1, k) - \frac{3}{4}(1 - k)^{2/3}\right], \quad I_d(k) = 2I^2(1, k) I_0(1, k)$$

At first sight, the choice of the constant k seems to permit $I_\Omega(k)$, and accordingly also C_Ω, to take arbitrary values. We shall show that this apparent possibility is not realizable. Let us find the derivative $d\eta/d\xi$ at the point f of the extremal generator and determine C_Ω and C_d for a few characteristic values of k. By the second formula of (1.5), if $\eta = \eta_f = 1$, we have

$$\left(\frac{d\eta}{d\xi}\right)_f = I(1,k)(1-k)^{1/3} \tag{1.7}$$

If follows from the formula for $I(1,k)$ that $I(1,k)$ is a continuous function of k at $k = 1$. Consequently, the integral $I(1,k)$, being positive for $k \leq 1$, maintains its sign in a finite neighbourhood of the point $k = 1$ and at $k > 1$. In that neighbourhood, as is clear from Eq. (1.7), $(d\eta/d\xi)_f < 0$, that is, such extremals *if* approach the point f from above, having at $x < L$ segments with $r > R$, which are forbidden by the formulation of the problem. Besides the violation of the size constraint $r \leq R$, dictated by the formulation of the problem, Newton's formula is not valid on valid on the extremal *if* on the shadow side of the aforementioned segments; the condition for Newton's formula to be applicable in this problem is [2, 4, 5]

$$0 \leq \theta \leq \pi/2 \tag{1.8}$$

Thus, temporarily leaving aside the not yet excluded possibility of a change in the sign of the integral $I(1,k)$ for some $k = k_* > 1$, we must assume that the constant may take values $k \leq 1$. By Eq. (1.7), the extremal corresponding to $k = 1$ has a horizontal tangent at the point f. As shown below, such an extremal plays an important role in the solution of our problem. Lets us calculate the corresponding coefficients $C_{\Omega 1}$ and C_{d1}. For $k = 1$ formulae (1.6) give

$$C_{\Omega 1} = \frac{1}{2}, \quad C_{d1} = \tau^2 I_d(1) = 8\tau^2 I_0^3(1,1) \tag{1.9}$$

By the equality $I(1,1) = 2I_0(1,1)$ and the value found numerically for the integral $I_0(1,1)$, we find for the contour in a small neighbourhood of the leading point and for the coefficients $C_{\Omega 1}$ and C_{d1}

$$\xi \approx 0.73\eta^{4/3}, \quad C_{\Omega 1} = \frac{1}{2}, \quad C_{d1} = 1.0822\tau^2 = \frac{0.2706}{C_{\Omega 1}^2}\tau^2 \tag{1.10}$$

The constant $k = 0$ corresponds to $\lambda = 0$, which is equivalent to the problem of designing a "Newtonian" optimum nose shape for given τ in a free volume. The Newtonian nose shape has minimum drag, and the corresponding parameters are

$$\xi = \eta^{4/3}, \quad C_{\Omega 0} = \frac{2}{5}, \quad C_{d0} = \frac{27}{32}\tau^2 = \frac{27}{200C_{\Omega 0}^2}\tau^2 \tag{1.11}$$

Because of the differences in the definitions of C_d and τ, the coefficient 27/32 in the formula for C_{d0} is twice as large as the analogous coefficient obtained in [1].

By the formulae of (1.10) and (1.11), the slender-body condition is violated at the leading point, where $x' = \tau\xi' = \infty$, and in its neighbourhood. However, this has little influence on the drag of the entire nose shape, because in this case, by the second formula of (1.2), the contribution to C_d of the neighbourhood of a tip of relative radius η is small (proportional to $\eta^{4/3}$).

If the volume and base radius are given but the length of the nose shape is free, the coordinate x in the formulation of the variational problem must be in units not of L but of R, introducing a variable $\xi^\circ = x/R$. After that, τ in formulae (1.2) and (1.3) is replaced by 1, and ξ by ξ°. As a result, the condition determining the optimum length is obtained by equating the coefficient of $\delta\xi_i^\circ$ to zero in the otherwise unchanged expression (1.3) for $\delta\Phi$. This is equivalent to equating the constant of integration C in Eq. (1.4) to zero and letting the constant k in formula (1.5) equal "minus infinity." This last operation formally equivalent to replacing the quantities $(1-k\eta^2)$ and $(1-k\zeta^2)$ in (1.5) and (1.6) by η^2 and ζ^2, respectively. As a result, on returning to the variable $\xi = x/L = \tau\xi^\circ$, where, unlike the previous case, L is not a given quantity but an unknown length, we obtain

$$\xi = \eta^{2/3}, \quad C_{\Omega(-\infty)} = \frac{1}{4}, \quad C_{d(-\infty)} = \frac{27}{16}\tau^2 = \frac{27}{256C_{\Omega(-\infty)}^2}\tau^2 \tag{1.12}$$

Although by what has just been said the second formula of (1.12) serves to determine τ when $C_{\Omega(-\infty)}$ is given, it may also be used to determine the quantity $C_{\Omega(-\infty)}$, which for fixed τ corresponds to $k = -\infty$. Thus, by formulae (1.10)–(1.12), for any given τ, variation of k from 1 to $-\infty$ gives the values of τC_Ω for the optimum nose shapes in the range [1/4, 1/2]. On the other hand, corresponding to the condition (1.8) for the applicability of Newton's formula (1.1), we have the nose shapes from a trailing flat end: $x = L$, $0 \le r \le R$ to blunt cylinder: $x = 0$, $0 \le r \le R$; $0 \le x \le L$, $r = R$. The coefficient C_Ω for these varies from 0 to 1. True, the slender-body approximation becomes meaningless at a flat end ($x'^2 \gg 1$). However, even if this as yet mathematically unformulated restriction is taken into account, the difference between the interval [1/4, 1/2] we have found and the possible interval [0, 1] within which the coefficient C_Ω is varied, which is four times longer, indicates that the solution we have constructed is incomplete.

Remarks. 1. The reason for the aforementioned incompleteness is that the solution of the problem, whether here or in [1], disregarded certain constraints which are implicitly taken for granted but not automatically valid. Among these is constraint (1.8) on the inclination θ of the tangent to the generator, and the constraints on size,

$$0 \le r \le R, \quad 0 \le x \le L, \quad \text{or} \quad 0 \le \eta \le 1, \quad 0 \le \xi \le 1 \tag{1.13}$$

The first of these constraints was indeed used above, but only to reject k values in excess of unity.

2. When the design of optimum nose shapes is considered without any assumptions about their thinness, whether for given sizes [4] or for a given volume and base radius [5], the constraints (1.8) imposed on the angle and the length coordinate (1.13) play a decisive role. Because of them, the optimum contour in the first problem, for any τ values, contains a leading flat end [2–4] – a boundary extremum segment in the sense of both x and θ. The size of the flat end, which remains finite for finite values of τ, tends to zero as $\tau \to 0$. The obligatory appearance of a flat end in an optimum nose shape of the dimensions given has also been established when the problem is solved in the approximation of the complete Euler equations [6]. In the thin-body approximation, a "trace" of the flat end in the same problem is the vertical tangent to the contour of the nose shape at its leading point. In the second problem, with $0 \le C_\Omega/\tau < 13/30$, the same constraints lead to a flat end $x = L$ – a boundary extremum segment with a protruding sharp pin [2, 5]. In both problems, at the junction point of the extremal (a two-sided extremum segment) and the flat end one has $\theta = 45°$ on the extremal, but $\theta \le 45°$ at all points of the extremal. In the first problem, Legendre overlooked (or misunderstood) this last inequality, already obtained by Newton [3]. Instead, he established a weaker condition (Legendre's condition), $\theta \le 60°$. It has been shown [2] that, without the thin-body assumption, the same condition $\theta \le 45°$ must hold on the extremal even when the radial size and volume of the nose shape are given.

Remarks 1 and 2 hold when solving problems similar to that considered here, but without the slender-body assumption. Since, in view of the simplified version of formula (1.1), that assumption yields infinite pressure at $x' = 0$, this surely eliminates flat ends $x = 0$ and $x = L$ from the desired optimum nose shape. Under those conditions, in view of the constraints (1.13), the only possible remaining boundary extremum segments are the segment $r = 0$ or $\eta = 0$ of the axis of symmetry and the segment $r = R$ or $\eta = 1$ of the generator of cylinder. The conditions for their connection (at the point d in Fig. 1b) to the extremal (two-sided extremum segment) are derived from suitably formulated transversality conditions. These conditions, as can be shown, reduce to the requirement of smooth attachment, that is, the equality $(d\eta/d\xi)_d = 0$ at the initial or final point (for the upper or lower generator, respectively, in Fig. 1b) of the extremal. The volume and drag of the optimum nose shape with a contour containing a segment of the axis of symmetry id do not differ from their values for a nose shape which, corresponding to $k = -\infty$, is of length Ll for $0 \le l \le 1$. Therefore, by (1.12),

$$C_\Omega = \frac{l}{4}, \quad C_d = \frac{27}{16}\left(\frac{R}{Ll}\right)^2 = \frac{27\tau^2}{16l^2} = \frac{C_{d(-\infty)}}{l^2} = \frac{27\tau^2}{256C_\Omega^2}, \quad 0 \le l \le 1 \tag{1.14}$$

In fact, according to the formulation of the problem, the segment id of the axis of symmetry, which makes a zero contribution to both the volume and the drag of the nose, is also superfluous, since its removal does not violate the constraints (1.13) imposed on the maximum admissible length of the nose shape.

The drag of an optimum nose shape with contour containing the segment df of the straight line $r = R$ does not differ from that of a nose shape which, corresponding $k = 1$, is of length Ll, $0 \le l \le 1$, when the additional volume of its cylindrical part equals $\pi R^2 L(1 - l)$. Therefore, by formulae (1.9)

$$C_\Omega = 1 - \frac{l}{2}, \quad C_d = 1.0822\frac{\tau^2}{l^2} = \frac{0.2706\tau^2}{C_\Omega^2(2-l)^2 l^2}, \quad 0 \le l \le 1 \tag{1.15}$$

Formulae (1.14) yield the coefficient C_d of optimum nose shapes for $0 \le C_\Omega \le 0.25$, and formulae (1.15) do the same for $0.5 \le C_\Omega \le 1$. To the minimum ($C_\Omega = 0$) and maximum ($C_\Omega = 1$) possible volumes there correspond the value $l = 0$ and the same infinite drag coefficients C_d. This latter fact is the result of using Newton's formula (1.1) in the slender body approximation ($x'^2 \gg 1$) which is violated for any τ, however small, at flat ends $x = 0$ and $x = L$. But if the first (full) version of Newton's formula is used, the drag coefficients of the flat ends $x = 0$ and $x = L$, $0 \le r \le 1$, turn out to be finite, though a maximum ($C_d = 1$).

This fact, and the possibility of a vertical tangent at the leading point of nose shapes which are optimal in the slender-body approximation, justifies computing their drag coefficients with the complete Newton formula.

We will now present the equations of "thin" optimum contours and formulae for the coefficients C_Ω and C_d, as found above. All the contours begin at the axis of symmetry and reach the point $\xi = \eta = 1$.

Pointed contours beginning at $\zeta = 1 - l (0 \le l < 1)$

$$\xi = 1 - l + l\eta^{2/3}, \quad C_\Omega = \frac{l}{4} \le \frac{1}{4}, \quad \frac{C_d}{\tau^2} = 27\int_0^1 \frac{\zeta^3 d\zeta}{9\zeta\tau^2 + 4l^2}; \quad 0 \le l \le 1, \quad 0 \le \eta \le 1, \quad 1 - l \le \xi \le 1 \tag{1.16}$$

This yields a pointed contour of maximum admissible length when $l = 1$

$$\xi = \eta^{2/3}, \quad C_{\Omega-\infty} = \frac{1}{4}, \quad \frac{C_{d(-\infty)}}{\tau^2} = 27\int_0^1 \frac{\zeta^3 d\zeta}{9\zeta\tau^2 + 4}$$

Blunt contours beginning at $\xi = \eta = 0$ *with less than "Newtonian" coefficients* C_Ω

$$\xi = \frac{I(\eta, -k)}{I(1, -k)}, \quad 0 \le \xi \le 1, \quad 0 \le \eta \le 1, \quad 0 \le k \le \infty$$
$$C_\Omega = \frac{1}{I(1,-k)}\int_0^1 \frac{\eta^{7/3} d\eta}{(1 + k\eta^2)^{1/3}}, \quad \frac{C_d}{\tau^2} = 2I^2(1,-k)\int_0^1 \frac{(1 + k\eta^2)^{2/3}\eta d\eta}{I^2(1,-k)(1 + k\eta^2)^{2/3}\tau^2 + \eta^{2/3}} \tag{1.17}$$

The Newtonian contour, which also begins at $\xi = \eta = 0$, corresponds to $k = 0$. For it

$$\xi = \eta^{4/3}, \quad C_{\Omega 0} = \frac{2}{5}, \quad \frac{C_{d0}}{\tau^2} = 18\int_0^1 \frac{\eta d\eta}{9\tau^2 + 16\eta^{2/3}} \tag{1.18}$$

Formulae (1.17) *hold for blunt contours with coefficients* $C_\Omega > C_{\Omega 0} = 2/5$, *also beginning at* $\xi = \eta = 0$, *but with* k *replaced by* $-k$ *for* $0 \le k \le 1$. For $k = 0$ they reduce to formulae (1.18) for a Newtonian contour, and for $k = 1$ they describe a contour with a horizontal tangent at $\xi = \eta = 1$, for which

$$\xi = \frac{I(\eta, 1)}{I(1, 1)}, \quad 0 \le \xi \le 1, \quad 0 \le \eta \le 1, \quad C_{\Omega 1} = \frac{1}{2}, \quad \frac{C_{d1}}{\tau^2} = 2I^2(1,1)\int_0^1 \frac{(1-\eta^2)^{2/3}\eta d\eta}{I^2(1,1)(1-\eta^2)^{2/3}\tau^2 + \eta^{2/3}}$$

Blunt contours beginning at $\xi = \eta = 0$ *and having a cylindrical segment* $l \le \xi \le 1, \eta = 1$ $(0 \le l \le 1)$

$$\xi = l\frac{I(\eta, 1)}{I(1, 1)}, \quad 0 \le \eta \le 1, \quad 0 \le \xi \le l, \quad 0 \le l \le 1$$
$$C_\Omega = 1 - \frac{l}{2}, \quad \frac{C_d}{\tau^2} = 2I^2(1,1)\int_0^1 \frac{(1-\eta^2)^{2/3}\eta d\eta}{I^2(1,1)(1-\eta^2)^{2/3}\tau^2 + l^2\eta^{2/3}} \tag{1.19}$$

Hence, for $l = 1$ we obtain the previous contour, and for $l = 0$ a "full" cylinder with $C_\Omega = C_d = 1$.

2. OPTIMUM NOSE SHAPES IN THE APPROXIMATION OF THE COMPLETE NEWTON FORMULA

If the complete Newton formula is used and the maximum admissible radius of the nose R is taken as the scale of both coordinates, the formulae for the coefficients C_Ω and C_d become ($\eta' = d\eta/d\xi$, $\xi' = d\xi/d\eta$)

$$\frac{C_\Omega}{\tau} = \int\limits_{0,(\eta'>0)}^{1} \eta^2\xi' d\eta + \int\limits_{\eta'=0} \eta^2 d\xi, \quad C_d = 2\int\limits_0^1 \frac{\eta d\eta}{1+\xi'^2}, \quad \xi = \frac{x}{R}, \quad \eta = \frac{r}{R} \tag{2.1}$$

With this in mind, the Lagrange functional may be written as

$$\Phi = C_d + \lambda\frac{C_\Omega}{\tau} = 2\int\limits_0^1 \frac{\eta d\eta}{1+\xi'^2} + \lambda \int\limits_{0,\eta'>0}^{1} \eta^2\xi' d\eta + \lambda \int\limits_{\eta'=0} \eta^2 d\xi$$

and its variation can be evaluated:

$$\begin{aligned}\delta C_d = \delta\Phi = {} & Y_{t+}\Delta\eta_t - Y_{b-}\Delta\eta_b + [X_{t+} - X_{b-} + \lambda(\eta_b^2 - \eta_t^2)]\Delta\xi_t \mp Z_{d\pm}\Delta\eta_d \pm X_{d\pm}\Delta\xi_d + \\ & + \int\limits_{\eta'>0} (X - \lambda\eta^2)'\delta\xi d\eta + 2\int\limits_{\eta'=0} \lambda\eta\delta\eta d\xi + \int\limits_{\xi'\geq 0} G(\delta\xi')^2 d\eta + \\ & + \int\limits_{\xi'=0} [X_{b-} + \lambda(\eta^2 - \eta_b^2)]\delta\xi' d\eta\end{aligned} \tag{2.2}$$

$$X = \frac{2\eta\xi'}{(1+\xi'^2)^2}, \quad Y = \eta\xi'^2\frac{\xi'^2-1}{(1+\xi'^2)^2}, \quad Z = \eta\frac{1+3\xi'^2}{(1+\xi'^2)^2}, \quad G = \eta\frac{3\xi'^2-1}{(1+\xi'^2)^3}$$

where b and t are the lower and upper points of the possible flat end bt, minus and plus subscripts indicate values before and after the corresponding point (moving from i to f), the relations $\eta' > 0$, etc. indicate integration over sections with $\eta' > 0$, etc., and $\Delta\eta$ and $\Delta\xi$ are the increments of the coordinates of points at which different segments are attached.

Formulae (2.2) incorporate the terms written out in [2], where the variational problems were solved either with fixed sizes or with fixed radial size and volume; besides these terms, however, our formulae also include the integral over the cylindrical segments df with $\eta = 1$ and $\eta' = 0$, as well as terms containing $\Delta\eta_d$ and $\Delta\xi_d$. The latter appear in two cases: (1) if the optimum nose shape proves to be shorter than L; in that case, corresponding to the upper signs and subscripts in formulae (2.2), the generator begins on the axis of symmetry at a point i coinciding with d, and $\Delta\eta_d = 0$; (2) if the optimum nose shape contains a cylindrical segment $\eta = 1$; corresponding to this case in formulae (2.2) are the lower signs and subscripts, and in addition $\Delta\eta_d$ and $\delta\eta$ in the integrand of the integral over $\eta' = 0$ are non-positive.

Investigation of the terms on the right-hand side of the expression for δC_d in formula (2.2) yields the necessary conditions for C_d to be a minimum, thus defining the optimum generator *if*. On two-sided extremum segments (TSES), where the variations $\delta\xi$ are arbitrary, we have

$$\lambda\eta^2 - X \equiv \eta\left[\lambda\eta - \frac{2\xi'}{(1+\xi'^2)^2}\right] = C \tag{2.3}$$

with the constant of integration C suitably determined.

The requirement that the coefficient of $(\delta\xi')^2$ in formula (2.2) should be non-negative yields Legendre's necessary condition $\xi' \geq 1/\sqrt{3}$. This condition, however, turns out to be too weak, and it may be replaced by the aforementioned inequality

$$\xi' \geq 1 \tag{2.4}$$

Indeed, at any point of a TSES one can introduce an infinitesimal flat end bt for which $\Delta\eta_b \leq 0$, while $\Delta\eta_t \geq 0$ because the unvaried contour is smooth at that point. If condition (2.4) fails to hold, such increments $\Delta\eta_b$ or $\Delta\eta_t$ reduce the drag.

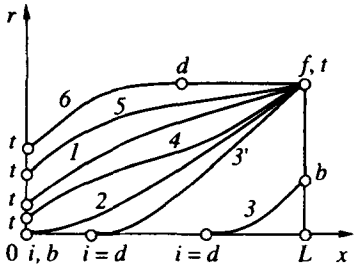

Fig. 2

Suppose the optimum contour contains a leading flat end ($\xi = 0$) or a trailing flat end ($\xi = L/R = 1/\tau$) which, because of the constraints (1.8) and (1.13), as previously [2–5], may appear as boundary extremum segments simultaneously in the sense of the both θ and ξ. At the points where they attach to the TSES, the increments $\Delta\eta_b$ or $\Delta\eta_t$ are arbitrary. Consequently, as in [2–5], the following equalities must hold at the point b and t

$$\xi'_{b-,\,t+} = 1 \tag{2.5}$$

that is, the TSES approach any flat end at an angle of 45°.

Different types of non-slender optimum axisymmetric nose shapes are shown in Fig. 2. They all differ in shape: "pointed" (contours *2*, *3*, *3'*) with $\xi'_{i,\,d} = \infty$; with leading flat end (*1*, *4–6*), with a trailing flat end (*3*) and without a trailing flat end (*1*, *2*, *3'*, *4*, *5* and *6*); in addition, they may have a cylindrical segment (*6*). For contours with a leading flat end , the points b and i coincide, but since the former adjoins the axis of symmetry of the left, $\xi'_{b-} = \infty$. For contours with a trailing flat end, the point t coincides with f.

For each fixed aspect ratio or $\tau = R/L$, the least drag is obtained with a blunt nose shape *1*, corresponding to Newton's problem [2–4] with free volume. To construct it, the multiplier λ in Eq. (2.3) must be equated to zero. As a result, owing to condition (2.5) at the point t, the equation of the Newtonian TSES is found to be

$$\frac{\eta\xi'}{(1+\xi'^2)^2} = \frac{\eta_t}{4} \tag{2.6}$$

Taking the parameter to be $q = \xi'$ as in [1–6], we integrate Eq. (2.6), observing the conditions at the point d and f. After computing $C_\Omega = C_{\Omega 0}$ and $C_d = C_{d0}$, we obtain

$$\eta = \eta_t\frac{(1+q^2)^2}{4q}, \quad \xi = \frac{\eta_t}{16}(3q^4+4q^2-7-4\ln q), \quad 1 \le q \le q_f, \quad \eta_t = \frac{4q_f}{(1+q_f^2)^2}$$

$$\frac{C_{\Omega 0}}{\tau} = \frac{(q_f^2-1)(18q_f^{10}+123q_f^8+373q_f^6+673q_f^4+823q_f^2-30)-120q_f^2\ln q_f}{60(1+q_f^2)^6}q_f \tag{2.7}$$

$$C_{d0} = \frac{3q_f^6+10q_f^4+17q_f^2+4q_f^2\ln q_f+2}{2(1+q_f^2)^4}, \quad \tau = \frac{4(1+q_f^2)^2}{q_f(3q_f^4+4q_f^2-7-4\ln q_f)}$$

If $q_f^2 \gg 1$, then $q^2 \gg 1$ on the larger segment of the extremal and, because of the different definition of ξ, the equation of the extremal and the formulae for $C_{\Omega 0}$ and C_{d0} derived from formulae (2.7) are identical with the equations and formulae (1.11).

For any non-zero τ, for values of C_Ω note exceeding a certain quantity C_Ω^m, the optimum contours are short contours with $\xi_i = \xi_d > 0$ and pointed contours ($\xi'_{i+} = \infty$) for $\tau > 1/2$ with trailing flat end (type *3*), and for $\tau \le 1/2$ with or without trailing flat end (curve *3* and curves of type *2* with trailing flat end). Indeed, in such cases the sign of $\Delta\xi_d$ is arbitrary. Therefore, one of the conditions for optimality is that the coefficient of X_{d+} in Eq. (2.2) should vanish. This yields $\xi'_{d+} = 0$ and $\xi'_{d+} = \infty$, but $\xi'_{d+} = 0$ does not satisfy the necessary condition (2.4). Consequently, $\xi'_{d+} = \infty$, and pointed nose shapes are

optimal. For them, one has $C = 0$ in Eq. (2.3), and in the case of a trailing flat end, the following holds on the extremal

$$\eta = \frac{2\xi'}{\lambda(1+\xi'^2)^2} = \frac{4\eta_b q}{(1+q^2)^2} \tag{2.8}$$

where the multiplier λ is expressed in terms of η_b using Eq. (2.5), which is in that case true at the point b. Equation (2.8) is integrated in the same way as (2.6). As a result one obtains, as in [2. 5]

$$\eta = \frac{4\eta_b q}{(1+q^2)^2}, \quad \xi = \frac{1}{\tau} + 2\eta_b\left[\frac{1+3q^2}{(1+q^2)^2} - 1\right], \quad 1 \le q \le \infty, \quad \eta_{i=d} = 0, \quad \xi_{i=d} = \frac{1}{\tau} - 2\eta_b$$
$$\frac{C_\Omega}{\tau} = \frac{13}{30}\eta_b^3, \quad C_d = 1 - \frac{13}{20}\eta_b^2 = 1 - \frac{1}{2}1.3^{1/3}\left(\frac{3C_\Omega}{\tau}\right)^{2/3} \approx 1 - 1.135\left(\frac{C_\Omega}{\tau}\right)^{2/3} \tag{2.9}$$

For fixed τ, the solution (2.9) holds for values of η_b that satisfy the inequality

$$0 \le \eta_b \le \eta_b^m = \inf[1, 1/(2\tau)] \tag{2.10}$$

The contours (2.9) are not slender over such substantial segments, but unlike solution (2.7), they have no analogues among contours designed in the slender-body approximation.

If the second part of condition (2.10) is true with the sign "smaller than" and for coinciding points b and f, that is, if $\tau < 1/2$, then for such τ, over a finite range of values of the coefficients $C_\Omega/\tau > 13/30$, the optimum nose shape length will also be less than L. Unlike those already considered, in these nose shapes without a trailing flat end the inclination of the tangent at the point f_- is less than 45° and consequently $q_f > 1$. For such contours, formulae (2.9) are replaced by

$$\eta = \frac{q(1+q_f^2)^2}{q_f(1+q^2)^2}, \quad \xi = \frac{1}{\tau} - \frac{1+3q_f^2}{2q_f} + \frac{(1+q_f^2)^2(1+3q^2)}{2q_f(1+q^2)^2}, \quad 1 < q_f \le q \le \infty$$
$$\frac{C_\Omega}{\tau} = \frac{45q_f^4 + 6q_f^2 + 1}{2^3 \cdot 15q_f^3}, \quad C_d = \frac{15q_f^2 - 1}{20q_f^2(1+q_f^2)} \tag{2.11}$$

Hence, in particular, for a given $\tau < 1/2$ one can find the maximum $q_f^m > 1$ and, using that value, the maximum $C_\Omega^m/\tau > 13/30$ for which optimum pointed nose shapes without a trailing flat end defined by these formulae have a length L (curve *2* in Fig. 2). Namely, writing out the second equation to (2.11) at the point i, where $\xi_i = 0$ and $q_i = \infty$, we obtain a quadratic equation whose solution gives

$$q_f^m = \frac{1}{3}\left(\frac{1}{\tau} + \sqrt{\frac{1}{\tau^2} - 3}\right) \tag{2.12}$$

If the pointed nose shape described by formulae (2.11) is slender, that is, $\tau \ll 1$, but $q_f \gg 1$, it can be shown using these inequalities that (taking account of the different scaling of the longitudinal coordinate) formulae (2.11) reduce to (1.12).

The solutions (2.11), which yield nose shapes of length not exceeding the maximum admissible length L, do not depend on the latter. Everything proved previously [2, 5] for nose shapes that are optimal with respect to fixed volume and base radius remains valid for such shapes also. According to those results, the generators are concave. On the other hand, the generator of a Newtonian nose shape (curve *1* in Fig. 2) is convex [2–5]. For fixed τ, therefore, the volume $C_{\Omega 0}$ of a blunt nose shape (see the formula for $C_{\Omega 0}$ in (2.7)) necessarily exceeds the volume C_Ω^m of the pointed concave nose shape defined by the penultimate equation of (2.11), which corresponds to the same value of τ and the value of q_f^m defined from that value by formula (2.12). If $C_\Omega > C_\Omega^m$, the contours of the optimum nose shapes have leading flat ends and end at the point f with a finite inclination of the tangent (of the type of curves *4* and *5* in Fig. 2). The shape of their TSES is defined by Eq. (2.2) with a constant $C \neq 0$. As above, it is integrated by introducing a parameter q with $1 = q_{t+} \le q \le \infty$. Having solved Eq. (2.3) – a quadratic equation in $\eta = \eta(q)$ – for that case, we find

$$\eta^{\pm}(q) = \frac{1}{\lambda}\left[\frac{q}{(1+q^2)^2} \pm \sqrt{\frac{q^2}{(1+q^2)^4} + \lambda C}\right]$$
$$\lambda = \left[\frac{2q_f}{(1+q_f^2)^2} - \frac{\eta_t}{2}\right]\frac{1}{1-\eta_t^2}, \quad C = \left[\frac{2q_f\eta_t}{(1+q_f^2)^2} - \frac{1}{2}\right]\frac{\eta_t}{1-\eta_t^2} \tag{2.13}$$

The Newtonian optimum nose shape corresponds to $\lambda = 0$. As $\lambda \to 0$, one obtains finite η values if the minus sign is taken in the first equation of (2.13). For any τ, therefore, convex optimum contours, including some similar to Newtonian contours, are obtained for $\eta = \eta^-(q)$. For them

$$\eta = \eta^-(q), \quad \xi = q\eta - \eta_t - \int_1^q \eta^-(q)dq, \quad 1 \le q \le q_f; \quad \frac{1}{\tau} = q_f - \eta_t - \int_1^{q_f} \eta^-(q)dq$$
$$\frac{C_\Omega}{\tau} = \frac{q_f - \eta_t^3}{3} - \frac{1}{3}\int_1^{q_f} [\eta^-(q)]^3 dq, \quad C_d = \frac{1}{2}\eta_t^2 + \frac{1}{1+q_f^2} + 2\int_1^{q_f} \frac{[\eta^-(q)]^2 q dq}{(1+q^2)^2} \tag{2.14}$$

Since corresponding to the equality $C_\Omega^m = C_{\Omega 0}$ one has a pointed concave generator *if*, it follows that when $C_\Omega < C_{\Omega 0}$ decreases the optimum generators must become convex-concave with convex initial segment and concave end segment. It can be shown that at the point of inflection separating these segments, the expression under the radical sign in formula (2.13) vanishes, and q takes its maximum value for the contour, q^m. Thus, at the point of inflection

$$\varphi(q^m) \equiv \frac{q^{m2}}{(1+q^{m2})^4} = -\lambda C \tag{2.15}$$

Moreover $1 < q_f \le q^m$, and $\varphi(q^m)$ decreases monotonically for $q^m > 1$ and vanishes at $q^m = \infty$. Accordingly, q^m as a function of λC is determine by rapidly convergent iterations (k is the number of the iteration)

$$z_{k+1}^3 = z_k^3\left[1 - \frac{1}{(1+z_k)^4}\right] - \lambda C, \quad q^m = \frac{1}{\sqrt{z}}, \quad z_0 = 1 \tag{2.16}$$

When $q_f = q^m$, the point of inflection coincides with the end point f. For a Newtonian solution $\lambda = 0$, and the value of q^m determined by formula (2.15) or by iterations (2.16) will equal infinity, so that the equality $q_{f0} = q^m$ will naturally not hold. Accordingly, the solution (2.14) holds within limits from $q_f = q_{f0}$ to the first point where $q^m = q_f$. Then all the integrals with respect to q split into two: from 1 to q^m, and from q^m to q_f (or to q), $\eta = \eta^-(q)$ in the first and with $\eta = \eta^+(q)$ in the second

$$\eta = \eta^-(q), \quad \xi = q\eta^-(q) - \eta_t - \int_1^q \eta^-(q)dq, \quad 1 \le q \le q^m$$
$$\eta = \eta^+(q), \quad \xi = q\eta^+(q) - \eta_t - \int_1^{q^m} \eta^-(q)dq + \int_q^{q^m} \eta^+(q)dq, \quad q^m \ge q \ge q_f$$
$$\frac{1}{\tau} = q_f - \eta_t - \int_1^{q^m} \eta^-(q)dq + \int_{q_f}^{q^m} \eta^+(q)dq, \quad \frac{C_\Omega}{\tau} = \frac{q_f - \eta_t^3}{3} - \frac{1}{3}\int_1^{q^m} [\eta^-(q)]^3 dq + \tag{2.17}$$
$$+ \frac{1}{3}\int_{q_f}^{q^m} [\eta^+(q)]^3 dq, \quad C_d = \frac{\eta_t^2}{2} + \frac{1}{1+q_f^2} + 2\int_1^{q^m} \frac{[\eta^-(q)]^2}{(1+q^2)^2} q dq - 2\int_{q_f}^{q^m} \frac{[\eta^+(q)]^2}{(1+q^2)^2} q dq$$

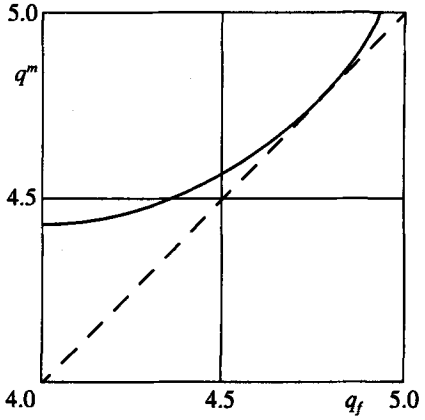

Fig. 3

Figure 3 illustrates the transition from convex optimum contours to convex-concave ones. The thick curve represents the function $q^m = q^m(q_f)$ for $\tau = 1/4$. For such τ, by the last formula of (2.7), $q_f \equiv q_{f0} \approx 5.48$. As mentioned before, $q^m(q_{f0}) = \infty$. The optimum TSES for $4.75 \le q_f \le q_{f0}$ are convex. To construct them one first uses the third equation of (2.14) to determine $\eta_t = \eta_t(q_f)$, then finding $\lambda = \lambda(q_f)$ and $C = C(q_f)$ from formulae (2.13), and finally $q^m = q^m(q_f)$ from Eqs (2.15) and (2.16). Corresponding to the point at which the curve is tangent to the dashed straight line $q^m = q_f$ is an optimum contour whose curvature vanishes at its end point. For lower q_f values one has convex-concave optimum generators. To compute them, one first determines $q^m(q_f)$, $\lambda(q_f)$ and $C(q_f)$ by simultaneous solution of Eq. (2.15) and the fifth equation of (2.17) with $\eta^{\pm}(q)$, λ and C from formulae (2.13). By Fig. 3, to the left of the point of tangency one has $q^m(q_f) > q_f$. Now, however, unlike the right branch, this is a natural consequence of the presence of an optimal generator of a concave trailing segment. As $q_f \to q_f^m$, where for $\tau = 1/4$, by Eq. (2.12), $q_f^m \approx 2.535$, the optimum contour with leading flat end tends, outside a small neighbourhood of the point, to a pointed contour of the same length. In that case, $\eta_t \to 0$, $q^m \to \infty$, but the value of q_{t+} remains constant (equal to unity).

For short nose shapes ($\tau > 1/2$), some of the optimum contours have two flat ends (leading and trailing), while the TSES joining them consists of convex (leading) and concave (trailing) segments. At the point b where the extremal attaches to the trailing flat end, $\eta_b < 1$, $q_{b-} = 1$. When designing such contours, q_f in the appropriate inequality of (2.17) should be replaced by 1, and formulae (2.13) for λ and C and the three last equalities of (2.17) are replaced by

$$\lambda = \frac{1}{2(\eta_b + \eta_t)}, \quad C = \frac{-\eta_b\eta_t}{2(\eta_b + \eta_t)}, \quad \frac{1}{\tau} = \eta_b - \eta_t + \int_1^{q^m} [\eta^+(q) - \eta^-(q)]dq$$

$$\frac{C_\Omega}{\tau} = \frac{\eta_b^3 - \eta_t^3}{3} + \int_1^{q^m} \frac{[\eta^+(q)]^3 - [\eta^-(q)]^3}{3} dq, \quad C_d = 1 + \frac{\eta_t^2 - \eta_b^2}{2} + 2\int_1^{q^m} \frac{[\eta^-(q)]^2 - [\eta^+(q)]^2}{(1+q^2)^2} q dq \tag{2.18}$$

For any τ and C_Ω over a finite range of values ($C_{\Omega\infty} \ge C_\Omega > C_{\Omega 0}$, where $C_{\Omega\infty}$ is defined below, and $C_{\Omega 0}$ for the same τ corresponds to a Newtonian nose shape) the optimum generators, as well as the Newtonian contour, have a leading flat end and a convex TSES ending at the point f (curves of type *5* in Fig. 2). Formulae (2.14) hold for these generators, with $q_{f0} < q_f \le \infty$. The coefficient $C_{\Omega\infty}$ corresponds to the optimum generator with a horizontal tangent at the point f, that is, with $q_f = \infty$. For this generator, by the last two formulae of (2.13)

$$2\lambda = 2C = -\eta_t(1 - \eta_t^2)^{-1} < 0 \tag{2.19}$$

For $1 \ge C_\Omega > C_{\Omega\infty}$, the optimum contour (curve *6* in Fig. 2) has, besides the leading flat end *it* and TSES *td*, a cylindrical boundary extremum segment *df*. In that case the sign of $\Delta\xi_d$ is arbitrary, and one

of the optimality conditions is that the coefficient X_{d-} in Eq. (2.2) should vanish. This occurs at $\xi'_{d-} = 0$ and $\xi'_{d-} = \infty$, but $\xi'_{d-} = 0$ does not satisfy condition (2.4). Therefore $\xi'_{d-} = \infty$ and the TSES *td* is attached to the cylindrical segment without a break. With this in view, the parametric notation for a TSES with a horizontal tangent at *f* may be represented in the form

$$\eta = \frac{q}{\lambda(1+q^2)^2} + \chi(q,\lambda), \quad \chi(u,\lambda) = \sqrt{\frac{u^2}{\lambda^2(q+u^2)^4} + 1}$$
$$\xi = 1 - \chi(1,\lambda) + \frac{q^2(1-q^2)}{2\lambda(1+q^2)^2} - q + q\chi(q,\lambda) - \int_1^q [\chi(u,\lambda) - 1]du, \quad 1 \le q \le \infty \tag{2.20}$$

Having written the second expression of (2.20) at the point *f*, we obtain

$$\frac{1}{\tau} = 1 - \chi(1,\lambda) - \frac{1}{2\lambda} - \int_1^\infty [\chi(u,\lambda) - 1]du \tag{2.21}$$

Given τ, one finds λ from Eq. (2.21) and, using λ, one employs Eq. (2.18) to find the η_t of the flat end. Then C_Ω and C_d may be computed from formulae (2.1) and with $\eta = \eta(q, \lambda)$ as in the first formula of (2.20), using the formulae

$$\frac{C_{\Omega\infty}}{\tau} = \frac{1-\eta_t^3}{3} + \frac{1}{3}\int_1^\infty (1-\eta^3)dq, \quad C_{d\infty} = \frac{1+\eta_t^2}{2} + 2\int_1^\infty \frac{\eta^2 - 1}{(1+q^2)^2} qdq \tag{2.22}$$

If, for fixed τ, the given volume Ω is such that $C_{\Omega\infty} < C_\Omega < 1$, then the optimum contour is a contour (curve *6* in Fig. 2) with leading flat end *it* and cylindrical end section *df* smoothly connecting with the TSES *td*. The TSES of the all such nose shapes are constructed by formulae (2.19)–(2.21) with the given value of τ replaced by a quantity τ° varying in the range $\tau < \tau^\circ \le \infty$. Formula (2.22) holds for finding the drag coefficients C_d of these nose shapes, after replacing τ by τ°, λ by λ°, η by η° and η_t by η_t°. Only the formula for C_Ω is modified: taking the volume of the cylindrical segment into account, that formula is written as

$$C_\Omega = C^\circ_{\Omega\infty} + \frac{\tau^\circ - \tau}{\tau^\circ}, \quad \frac{C^\circ_{\Omega\infty}}{\tau} = \frac{1-\eta_t^{\circ 3}}{3} + \frac{1}{3}\int_1^\infty (1-\eta^{\circ 3})dq, \quad \tau < \tau^\circ < \infty$$

The "degree" sign indicates quantities and functions defined by the previously presented formulae for $\tau^\circ > \tau$, and $\tau^\circ = \infty$ gives a blunt cylinder with $C_d = C_\Omega = 1$.

3. COMPUTATIONAL RESULTS

Some results of computations carried out with the solutions obtained above are in presented in Figs 4 and 5. Figure 4 illustrates contours with $\tau = 1/2$ and $\tau = 1/4$, which are optimal for different values of C_Ω, with the following correspondence of the contour numerals (labelling the curves), C_Ω values and drag coefficients C_d

№	1	2	3	4	5	6	7	8	9	10	11	12
C_Ω	0.014	0.22	0.44	0.59	0.86	0.007	0.11	0.24	0.41	0.52	0.72	0.93
C_d	0.90	0.35	0.16	0.21	0.46	0.90	0.35	0.10	0.049	0.063	0.15	0.46

Contour *1* for $\tau = 1/4$ yields as a short (aspect ratio less than the maximum admissible value $1/\tau = 2$) pointed nose shape with leading flat end, contour *2* yields a single pointed configuration for $\tau = 1/2$ of maximum admissible length with $q_f = 1$, and curve *3* yields a Newtonian nose shape with leading flat end. Curve *4* is the generator of a nose shape with leading flat end and TSES of maximum length with a horizontal tangent at the end point ($q_f = \infty$ for $\xi = 1/\tau = 2$). Finally, the nose shape *5* has two boundary extremum segments – a large leading flat end and a fairy long cylindrical generator $r \equiv R$.

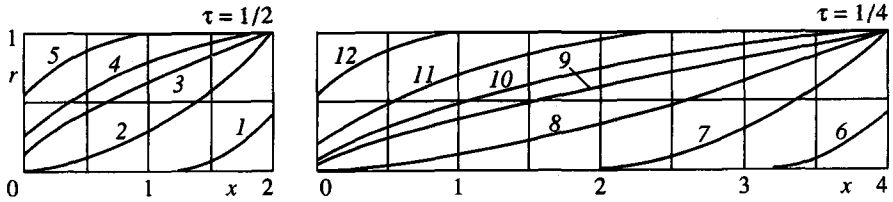

Fig. 4

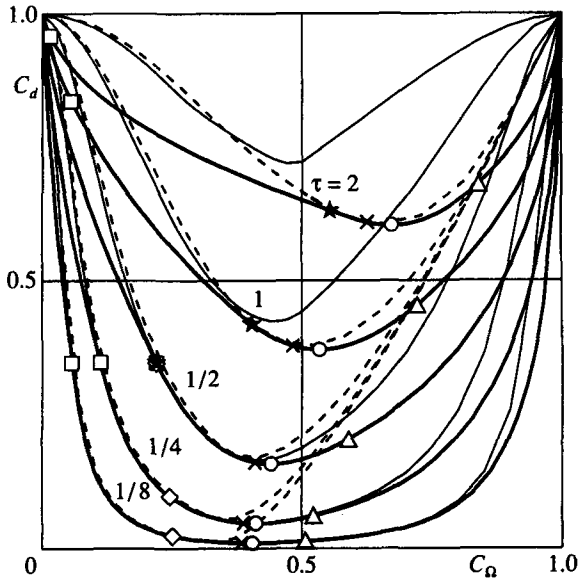

Fig. 5

For $\tau = 1/4$, the first two contours *6* and *7* are identical in shape and drag coefficients with contours *1* and *2*. The non-cylindrical initial segment of contour *7* coincides with contour *5* at $\tau = 1/2$, which implies that their drag coefficients are equal. The slender-body condition ($x'^2 \gg 1$) is satisfied over the entire pointed generator *8*. On the Newtonian contour *9*, on contour *10* with a TSES of maximum length and $q_f = \infty$, and on contour *11* with a horizontal section, the condition is violated only in a small neighbourhood (especially with respect to r^2) of the axis of symmetry. The drag of these bodies is close to that of nose shapes designed in the slender-body approximation.

The thick curves in Fig. 5 show the wave drag coefficients of the optimum nose shapes designed according to the results of Section 2 for $\tau = 1/8, 1/4, 1/2, 1, 2$, that is, for both large and small aspect ratios (from 8 to 1/2). For these τ values, the curves $C_d = C_d(\tau, C_\Omega)$ have been computed for all possible $0 \leq C_\Omega \leq 1$. The extreme values correspond to nose shapes with leading flat end ($C_\Omega = 1$) and trailing flat end ($C_\Omega = 0$) and the same $C_d = 1$ for any τ.

The marks on the thick curves indicate points corresponding to the characteristic solution listed above. The small circles represent Newtonian nose shapes which, for fixed τ, possess minimum drag (as they should). Between the circles and the triangles, the optimum nose shapes (for $C_{\Omega 0} < C_\Omega < C_{\Omega\infty}$) have a leading flat end and convex TSES. The triangles represent maximally thick nose shapes of this type with a horizontal tangent at the end point ($q_f = \infty$, $C_\Omega = C_{\Omega\infty}$). To the right of the triangles, the optimum contours consist of a leading flat end, convex TSES, and an end cylinder $r \equiv R$.

Between the circles and crosses the optimum generators ($C_\Omega < C_{\Omega 0}$) consist of convex TSES and leading flat end. At $\tau < 1/2$ the crosses represent contours for which the second derivative vanishes at the point *f*. For fixed τ values, to the left of the crosses up rhombi, the optimum contours consist of a leading flat end and a TSES with a point of inflection, and from the rhombi to the squares the optimum contours are concave, pointed, and without a trailing flat end ($q_i = \infty$, $\xi_i \geq 0$). The rhombi represent those of the latter nose shapes with full length, and the squares represent pointed contours with $q_f = 1$. At $\tau > 1/2$, from the crosses to the stars, the optimum contours consist of a leading flat end and

a TSES with a point of inflection; between the stars and the squares they consist of leading and trailing flat ends and a TSES with a point of inflection. The stars represent those of the latter nose shapes for which $q_f = 1$. At $\tau = 1/2$, the rhombus, square and star coincide ($C_\Omega = 13/60 \approx 0.22$). The sections of the thick curves to the left of the squares correspond to truncated nose shapes ($\xi_t > 0$) with concave, tapering TSES and trailing flat end.

The thin curves represent the function $C_d = C_d(\tau, C_\Omega)$ at $\tau = 1/8, 1/4, 1/2, 1$, for nose shapes that are optimum in the slender-body approximation, as defined by formulae (1.16)–(1.19), that is, the complete Newton formula. Naturally, for all τ the thin curves lie below the thick curves, but for $\tau \leq 1/2$ the thin and thick curves are close together over a certain range of C_Ω values, which becomes wider as τ decreases. As already noted, for the flats ends ($C_\Omega = 0$ and $C_\Omega = 1$) and similar configurations, the thin-body approximation is inapplicable, and computation of C_d in that approximation yields an unlimited increase in the wave drag coefficient. Formulae (1.16)–(1.19) eliminate the unlimited increase in C_d values. Moreover, when $C_\Omega = 0$ and $C_\Omega = 1$ the correct optimum configurations are defined solely by the size constraints, irrespective of the formulae used for the pressure. That is why both thin and thick curves begin and end at the same points. Nevertheless, as the distance from those points increases, the thin curves yield markedly larger C_d values than the thick ones. As τ decreases, such neighbourhoods become smaller. We recall that the equations and conditions obtained by Meile [1] permit the design of optimum nose shapes (in the slender-body approximation) only for $1/4 \leq C_\Omega \leq 1/2$.

The dashed curves in Fig. 5 represent the functions $C_d = C_d(\tau, C_\Omega)$ for pointed ($0 < C_\Omega \leq 1/3$) and blunted ($1/3 < C_\Omega \leq 1$) cones (with leading flat end $x = 0$). C_Ω increases from 0 to 1, the semi-aperture angle of the cones decreases monotonically from $\pi/2$ to 0. The coefficients C_Ω and C_d of the cones are defined by the following Formulae (as for optimum bodies, η_t is the size of the leading flat end in units of R)

$$C_\Omega = \frac{1 + \eta_t + \eta_t^2}{3} l, \quad C_d = \eta_t^2 + \frac{\tau^2 (1 + \eta_t)(1 - \eta_t)^3}{l^2 + \tau^2 (1 - \eta_t)^2}, \quad 0 \leq \eta_t \leq 1, \quad 0 \leq l \leq 1$$

The characteristics of the pointed cones are given by these formulae with $\eta_t = 0$ and $0 < l \leq 1$, and those of the blunted cones with $l = 1$ and $0 < \eta_t \leq 1$.

If $C_\Omega > 0.4$, then by Fig. 5 the drag of the blunted cones for $\tau \leq 1/2$ (the dashed curves) significantly exceeds that of optimum nose shapes according to the slender-body approximation (the thin curves). When $\tau \geq 1$ the situation is reversed, which is natural, since for such τ the slender-body approximation is inapplicable over the whole range of C_Ω values.

4. THE DRAG OF NOSE SHAPES COMPUTED BY INTEGRATING EULER'S EQUATIONS

In the light of previous results [6], it is natural to expect that for $C_{\Omega 0} \leq C_\Omega \leq 1$ the optimum contours obtained within the limits of Euler's equations should be analogous, that is, convex with leading flat end and with or without a cylindrical segment. At the same time, it seems interesting to design optimum nose shapes within the limits of the Euler, Navier-Stokes, and Reynolds equations for lower volume coefficients, for which the optimum contours obtained in the approximation of the complete Newton formula have a point of inflection and a leading flat end, as well as pointed contours without a leading flat end and with or without a trailing flat end. In these contours, all or a significant part of the generators that are optimal in the sense of Newton's formula are concave. In the flow of a gas – even an ideal gas – around concave generators (especially when there is a trailing flat end), separation is very probable. Under those conditions, when a scheme close to Newton's is used, the flow will take place not around the initial "solid" generator but around a similar "effective" contour, thus in principle modifying the results obtained when the model adopted assumes that the flow does not separate.

To ascertain the degree to which Newton's formula is applicable to the treatment of these problems, let us compare the drag coefficients obtained using that formula with those found by integrating Euler's equations with the same program as in [6].

Contours of different types were compared: long ($\tau = 1/8, 1/4, 1/2$) and short ($\tau = 1, 2$) convex (including those with horizontal end segment), short ($\tau = 1, 2$) with trailing flat end, and long ($\tau = 1/4$) concave pointed bodies. The results of the computations are presented in the table. Apart from the coefficient C_d, and geometrical characteristics: τ, C_Ω, upper ordinates of the leading end (η_t), lower ordinates of the trailing flat end (η_b), and left abscissae of the cylindrical segment ($\xi_d \leq 1$) of the optimum nose shapes (index "opt"), table 1 also lists the analogous values computed for pointed ($\eta_t = 0$) and

Table 1

№	τ	C_Ω	η_{tcon}	η_{topt}	ξ_{dopt}	η_{bopt}	C_{doptN}	C_{doptE}	$\frac{C_{doptN}}{C_{dconN}}$	$\frac{C_{doptE}}{C_{dconE}}$
1	1/8	0.70	0.66	0.03	5/8	1	0.043	0.045	0.100	0.122
2	1/4	0.72	0.69	0.17	3/5	1	0.146	0.134	0.300	0.327
3	1/2	0.73	0.70	0.38	5/8	1	0.304	0.250	0.607	0.583
4	1	0.74	0.71	0.57	1	1	0.474	0.371	0.872	0.815
5	2	0.84	0.83	0.76	1	1	0.684	0.528	0.949	0.894
6	1/2	0.22	0	0	1	1	0.350	0.449	0.943	1.120
6'	1/2	0.22	0	0	1	1	0.350	0.453	0.943	1.195
7	1	0.22	0	0.07	1	0.82	0.594	0.899	0.857	1.234
8	2	0.28	0	0.29	1	0.75	0.742	0.731	0.878	0.943

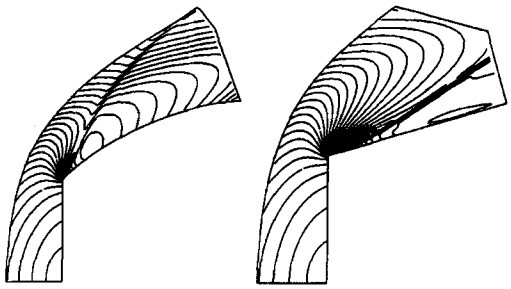

Fig. 6

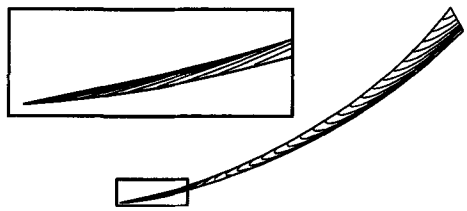

Fig. 7

blunted ($\eta_t > 1$) cones (index "con") with the same C_Ω values and maximum admissible τ (pointed cones with the same C_Ω values had lower τ values). The wave drag coefficients determined by Newton's formula and by Euler's equations are indicated by N and E, respectively.

The first five rows of the table correspond to values of τ and C_Ω for which the optimum Newtonian nose shapes have a convex generator, a leading flat end, and either include (rows 1–3) or do not include (rows 4 and 5) a cylindrical end segment. In the approximation of Euler's equations, flows around the Newtonian nose shapes in rows 1–8 and the blunted cones equivalent to them with respect to the value of the coefficient C_Ω and the maximum admissible values of τ were computed for a perfect gas with adiabatic exponent $\kappa = 1.4$ and free-stream Mach number $M_\infty = 5$. Figure 6 shows typical flow patterns around Newtonian (left) and "conical" (right) nose shapes. The isomach curves are drawn with $\Delta M = 0.1$. In flow around a blunted cone a trapped local separation occurs behind the break, as well as a strong oblique shock. The drag coefficients listed in the first five rows of the table, found by different methods, confirm the effectiveness of Newton's formula in designing convex optimum nose shapes.

Unlike flow around convex nose shapes, even non-separating flow of an ideal gas around concave optimum Newtonian nose shapes (rows 6 of the table and Fig. 7, $\Delta M = 0.1$, upper break at $M = 1.7$) and around equivalent cones is such that $C_{dconE} < C_{doptE}$. This situation does not change on changing to $M_\infty = 10$ and $\kappa = 1.1$. Results for these M_∞ and κ values are listed in row 6 of the table. The situation is even worse in the flow of an ideal gas around a comparatively slender body with trailing flat end (row 7),

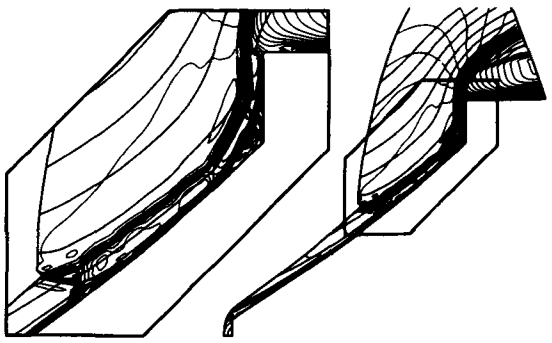

Fig. 8

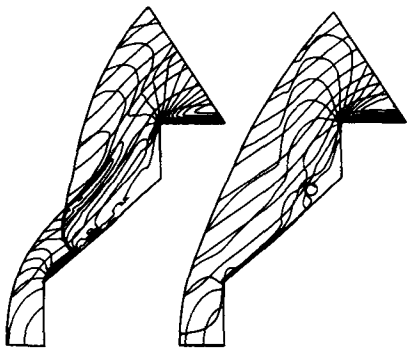

Fig. 9

which exhibits the formation of a complex shock wave system (Fig. 8). An important element of that system is a shock wave detached from the trailing flat end and interacting with an oblique front shock (at the triple point) formed in flow around a slightly blunted spike. An oblique shock of the weak family goes from the triple point toward the body. Supersonic flow toward the body behind this shock, after deflection in the reflected shock, as in one of the configurations investigated in [7] (see also [8–12]), forms a low-entropy wall jet with high impact pressure. The result is high pressure at the trailing flat end and a high value of $C_{d\text{opt}E}$. This case differs from the flows studies in [7–12] in the appearance at the wall of a thin high-entropy jet passing through the almost normal shock upstream of the leading flat end. The appearance of this jet causes the flow to separate near the point where the oblique shock impinges upon it and the point where the TSES attaches to the trailing flat end. High-entropy gas filling and evacuating these separation zones is one mechanism for the unsteady oscillations arising in flow around such bodies. Figure 8 is a "snapshot" of the flow, and $C_{d\text{opt}E}$ in the table is the coefficient averaged over time.

As τ is increased, the optimum Newtonian nose shape with two flat ends (row 8) turns out, even in the approximation of Euler's equations, to be slightly superior to the equivalent cone. However, as in the case of the body of row 7, separating flow around it is unsteady. This is illustrated in Fig. 9, which represents two instantaneous pictures of isomachs and particle trajectories (curves tangent to the velocity vector).

The dynamics of the transient depends on the number of the cells N in the difference grid. In the example, steady flow was obtained only with the coarsest grid ($N = 2^6$), that is, with high schematic viscosity. Intense oscillations were observed in grids with $N = 2^8, 2^{10}, 2^{12}, 2^{14}$. The time-averaged values of $C_{d\text{opt}E}$ for these grids were 0.757, 0.704, 0.704, 0.729.

5. CONCLUSION

Computations of optimum Newtonian nose shapes with $0 \leq C_\Omega < C_{\Omega 0}$ in an ideal gas flow, which are of interest in themselves, imply the urgent need to analyse the formulation of the initial variational problem. In practice, specification of the volume of the nose shape Ω (or, what is the same thing, the

coefficient C_Ω) is conditional either on the need to place several objects (the "working load", "instruments", etc.) of fixed total volume Ω_f in the nose, or on specification of the mass m_f of the working load. Obviously, for the placement of a load of given volume Ω_f, the volume Ω must satisfy the inequality $\Omega \geq \Omega_f$. If $\Omega_f \leq \Omega_0$, where Ω_0 corresponds to the solution of Newton's problem with free volume, this will yield the solution of the problem. If the specification of m_f defines the distance or final speed of the aircraft, the mass of the nose section m will satisfy the inequality $m \leq km_f$ with a given constant k exceeding unity. This, as it were, imposes an upper limit $\Omega \leq \Omega_f = km_f/\rho$ on the volume of the nose section, where ρ is some effective density of the working load. If $\Omega_f \leq \Omega_0$, however, that is not the case, because then a nose section with $\Omega = \Omega_0$ may be made partially empty, and the solution again reduces to the solution of Newton's problem with free volume. As a result, as can be seen in Fig. 5, when $\Omega_f \leq \Omega_0$ a significant reduction in the drag may be obtained (by a significant factor if $\tau \geq 1$).

We are grateful to N. I. Tillyayeva, who noticed an incompleteness in the solution of [1] when trying to use it in tests of a genetic optimization algorithm.

This research was supported financially by the Russian Foundation for Basic Research (02-01-00422 and 05-01-00846) within the framework of the "State Support for Leading Scientific Schools" programme (Nsh-2124.2003.1).

REFERENCES

1. MIELE, A., Slender bodies of minimum wave drag. In *Theory of Optimum Aerodynamic Shapes* (Edited by A. Miele). Academic Press, New York, 1965.
2. KRAIKO, A. N., PUDOVIKOV, D. Ye. and YAKUNINA, G. Ye., *Theory of Close to Optimal Aerodynamic Shapes*. YANUS-K, Moscow, 2001.
3. NEWTON, I., *Mathematical Principles of Natural Philosophy* (*Philosophiae naturalis principia mathematica*). University of California Press, Berkeley, CA, 1947.
4. KRAIKO, A. N., The determination of bodies of minimum drag using the drag laws of Newton and Busemann. *Prikl. Mat. Mekh.*, 1963, **27**, 3, 484–495. Gas Dynamics. Selection Vol. 1 (Edited by A. N. Kraiko). Fizmatlit, Moscow, 2000, 381–393.
5. KRAIKO, A. N., The nose section of given volume, optimum with respect to wave drag in the approximation of Newton's drag law. *Prikl. Mat. Mekh.*, 1991, **55**, 3, 382–388. Gas Dynamics Selection. Vol. 1 (Edited by A. N. Kraiko). Fizmatlit, Moscow, 2000, 394–402.
6. KRAIKO, A. N., PUDOVIKOV, D.Ye., P'YANKOV, K. S. and TILLYAYEVA, N. I., Axisymmetric nose shapes of specified aspect ratio, optimum or close to optimum with respect to wave drag. *Prikl. Mat Mekh.*, 2003, **67**, 5, 795–828.
7. EDNEY, B. E., Anomalous heat transfer and pressure distribution on blunt bodies at hypersonic speeds in the presence of an impinging shock. Aeronautical Research Institute of Sweden, Stockholm, 1968, FFA Rep. 115.
8. TANNEHILL, J. C., HOLST, T. L. and RAKICH, J. V., Numerical computation of two-dimensional viscous blunt body flows with an impinging shock, *AIAA Journal*, 1976, **14**, 2, 204–211.
9. TANNEHILL, J. C., HOLST, T. L., RAKICH, J. V. and KEYES, J. W., Comparison of two-dimensional shock impingement computation with experiment. *AIAA Journal*, 1976, **14**, 4, 539–541.
10. TANNEHILL, J. C., VIGNERON, Y. C. and RAKICH J. V., Numerical solution of two-dimensional turbulent blunt body flows with an impinging shock. *AIAA Journal*, 1979, **17**, 12, 1289–1290.
11. TILLYAYEVA, N. I., Extension of S. K. Godunov's scheme to arbitrary non-regular grids. *Uch. Zap. TsAGI*, 1986, **17**, 2, 18–26. Gas Dynamics. Selection, Vol 2 (Edited by A. N. Kraiko *et al.*). Fizmatlit, Moscow, 2001, 302–210.
12. GANZHELO, A. N., KRAIKO, A. N., MAKAROV, V. Ye. and TILLYAYEVA, N. I., Improving the accuracy of the solution of gas-dynamics problems. In *Current Problems of Aeromechanics. Collection of Papers*. Mashinostroyeniye, Moscow, 1987, 87–102.

Translated by D.L.